Journal of Applied Polymer Science

Combining Molecular Imprinted Nanoparticles with Surface Plasmon Resonance Nanosensor for Chloramphenicol Detection in Honey

Meryem Kara,[1] Lokman Uzun,[2] Sevgi Kolayli,[1] Adil Denizli[2]
[1]Department of Chemistry, Karadeniz Technical University, 61080 Trabzon, Turkey
[2]Department of Chemistry, Hacettepe University, 06381 Ankara, Turkey
Correspondence to: A. Denizli (E-mail: denizli@hacettepe.edu.tr)

ABSTRACT: The focus of this article is to develop a surface plasmon resonance (SPR) nanosensor to determine chloramphenicol (CAP) using the molecularly imprinted nanoparticles. The CAP imprinted nanoparticles were prepared by miniemulsion polymerization method. Then, the nanoparticles were attached onto the SPR nanosensor surface via temperature-controlled evaporation. Surface characterization studies were performed with atomic force microscopy and contact angle measurements. Kinetic studies were performed with CAP solutions in the concentration range of 0.155–6.192 n*M*. Florphenicol (FLP) and thiamphenicol (TAP) having similar chemical structures to the template (i.e., CAP) were chosen as competitors to determine selectivity of the nanoparticles. Selectivity constants were observed as 8.86 for CAP/TAP and 8.36 for CAP/FLP. The detection limit was calculated as 40 ng/kg honey sample. In the light of these results, it was emphasized that the SPR nanosensor is able to recognize CAP selectively and has a potential for real-time CAP detection in honey sample. © 2013 Wiley Periodicals, Inc. J. Appl. Polym. Sci. 129: 2273–2279, 2013

KEYWORDS: emulsion polymerization; molecular imprinting; nanoparticles; SPR nanosensor; food safety

Received 15 July 2012; accepted 9 December 2012; published online 17 January 2013
DOI: 10.1002/app.38936

INTRODUCTION

Chloramphenicol (CAP), a broad-spectrum bacteriostatic antimicrobial drug, exists as color scale of white to grayish-white or yellowish-white fine crystalline powder, needles, or elongated plates, with a melting point of 150.5–151.5°C.[1] It is active against rickettsia and chlamydophilia infections, the majority of obligate anaerobes, most gram-positive aerobes, and nonenteric aerobes, Enterobacteriacea.[2] CAP is used to combat against wide range of microbial infections including typhoid fever, meningitis, and certain infections of the central nervous system. However, there are various reports on that CAP can cause bone marrow depression, aplastic anemia, and leukemia.[3] According to regulation (EC) No. 1430/94, CAP is inserted in Annex IV (pharmacologically active substances for which no maximum levels can be fixed) and prohibited in food producing animals due to public health concerns.[4,5] Because of its high efficiency, broad spectrum activity, and relatively low cost, CAP is still illegally used for the treatment and prevention of some infectious diseases in animals, birds, bees, and shellfish.[6] Therefore, detection of CAP in food samples is considerably important for food safety requirements. European Community tries to uphold a high level of food standards to protect public health and safety[7] and has set up minimum required performance level at 0.3 μg/kg for CAP in food of animal origin.[8] Numerous methods such as enzyme linked immunosorbent assay,[9] liquid chromatography (LC), and LC-mass spectrometry (MS),[10] gas chromatography-mass spectrometry,[11] microbial assays,[12] capillary zone electrophoresis,[13] chemiluminescence,[14] biosensor-based immunoassay,[15] and immunoaffinity chromatography[16] have been used for the determination of CAP in different samples. Although good results were obtained with the methods mentioned, more sensitive, rapid, and new detection techniques are still required for CAP determination.

In recent years, surface plasmon resonance (SPR) sensor technology has become increasingly popular due to its properties such as robustness, sensitivity, versatility, delivering reliability, rapid, and relatively low-cost testing process.[17] Currently, SPR has been used in many areas such as diagnosis,[18] recognition of DNA,[19] enantiomeric compounds,[20] environmental monitoring,[21] food related applications,[17] and cell biology.[22] As one of the main optical sensor technologies, SPR sensors, have become a central tool for characterizing and quantifying molecular interactions[23] and permit real-time monitoring of chemical interactions without the need for labeling of reagents.[24] SPR sensors use surface plasmon waves to probe molecular interactions occurring at the surface of a sensor. It measures the

Additional Supporting Information may be found in the online version of this article.

change of refractive index by using a sensing surface coated with a thin layer of gold or silver film which is excited by a p-polarized light beam and so produces SPR signal.[25]

For SPR sensors, chip coatings use unstable/costly receptor molecules such as antibodies. These limitations have generated the need to investigate potential artificial recognizing elements.[26,27] Among artificial receptors, molecular imprinted polymers (MIPs) have proven their potential as synthetic receptors in numerous applications ranging from LC to sensor technology.[28–31] Molecular imprinting, which permits the formation of specific recognition and catalytic sites in polymer matrices, without elaborate designs, has been used extensively in the production of specific polymers with selective binding sites for a wide variety of molecules.[32]

There have been several reports for detection of CAP using MIPs and SPR technologies separately.[3,9–17] However, this study is one of the pioneer researches based on combination of MIP and SPR techniques in detection of CAP. In this study, we have prepared SPR nanosensor having CAP recognition sites by means of the MIP nanoparticles. To achieve this purpose, the CAP imprinted poly(ethylene glycol dimethacrylate-*N*-methacryloyl-L-histidine methylester) (PEDMAH) nanoparticles were synthesized via miniemulsion polymerization. Then, the PEDMAH nanoparticles were attached onto the surface of SPR nanosensor via temperature-controlled evaporation. Aqueous standard CAP solutions in different concentrations and honey samples were used for CAP detection studies. Kinetic and isotherm parameters were calculated by applying association kinetics analysis, Scatchard, Langmuir, Freundlich, and Langmuir-Freundlich isotherms. Florphenicol (FLP) and thiamphenicol (TAP) antibiotics were chosen as competitive components to determine the selectivity of nanoparticles. Finally, the ability of the SPR nanosensor for real-time CAP determination in honey sample was evaluated.

MATERIALS AND METHODS

Materials

CAP, TAP, FLP, poly(vinyl alcohol) (PVA, 87–90% hydrolyzed, average molecular weight 30,000–70,000, cold water soluble), sodium dodecyl sulfate (SDS), ammonium persulfate, sodium bicarbonate, sodium bisulfate, and potassium bromide (FTIR grade) were obtained from Sigma Chemical Co. (St. Louis, MO). *N*-Methacryloyl-L-histidine methyl ester (MAH), functional monomer for CAP coordination, was supplied from Nanoreg (Ankara, Turkey). Ethylene glycol dimethacrylate (EGDMA) and absolute methanol were purchased from Fluka A.G. (Buchs, Switzerland). All other chemicals used as received were of reagent grade and purchased from Merck A.G. (Darmstadt, Germany).

Preparation of CAP Imprinted PEDMAH Nanoparticles

Two-phase miniemulsion polymerization method was used to prepare the CAP imprinted PEDMAH nanoparticles.[33,34] Prior to polymerization, two different aqueous phases were prepared separately. The first aqueous phase was prepared by dissolving of PVA (200 mg), SDS (30 mg), and sodium bicarbonate (25 mg) in 10 mL of deionized water. The second phase was prepared by dissolving PVA (100 mg) and SDS (100 mg) in 200 mL of deionized water. MAH (5 mg) was dissolved in EGDMA (2.1 mL) to form organic phase. The organic phase was slowly added to the second aqueous phase. To obtain miniemulsion, the mixture was homogenized at 25,000 rpm by a homogenizer (T10, Ika Labortechnik, Germany). After homogenization, the template molecule (CAP, 10 μmol) was added to miniemulsion and the mixture was stirred for 2 h to obtain effectively interacted monomer–template prepolymerization complex. Then, the mixture was slowly added to the second aqueous phase while the phase has been stirring in a sealed-cylindrical polymerization reactor (250 mL). The reactor was magnetically stirred at 300 rpm (Radleys Carousel 6, UK). The polymerization mixture was slowly heated to 40°C, polymerization temperature. After that, nitrogen gas was bubbled through the solution for 5 min to remove oxygen dissolved in the solution. Then, the initiator pair, sodium bisulfite (125 mg) and ammonium persulfate (125 mg), were added into the solution. Polymerization was continued at 40°C for 24 h. The CAP imprinted nanoparticles were washed with water and water/ethanol mixtures, to remove unreacted monomers, surfactant, and initiators. For each washing step, the solution was centrifuged (Allegra-64R Beckman Coulter, Brea, CA, USA) at 30,000 rpm for 30 min; then, the nanoparticles were dispersed in fresh washing solution. At the last step, the CAP imprinted nanoparticles were dispersed in deionized water containing 0.3% sodium azide and stored at 4°C. The nonimprinted (NIP) nanoparticles were synthesized by applying same procedure except addition of the template molecule, CAP.

Characterization of CAP Imprinted PEDMAH Nanoparticles

The size distribution of nanoparticles was analyzed by zeta-sizer measurement. The experimental procedure for zeta-sizer is given as follows briefly: The nanoparticle samples (dispersed in 3 mL of deionized water) were immersed into sample holder of the zeta-sizer (NanoS, Malvern Instruments, London, UK). Light scattering was performed at incidence angle of 90° and 25°. For data analysis, density and refractive index of deionized water were taken as 1.00 g/mL and 1.33, respectively. Light scattering signal was calculated as nanoparticle number per second. Here, we have to mention that the nanoparticle concentration in sample was enough for measurement.

Preparation of CAP Imprinted SPR Nanosensor

Before attachment of the CAP imprinted nanoparticles onto the SPR nanosensor surface, gold surface of the SPR chip was cleaned with acidic piranha solution (3 : 1 H_2SO_4 : H_2O_2, v/v). The SPR chip was immersed in 20 mL of acidic piranha solution for 30 s. Then, it was washed with pure ethyl alcohol and dried in vacuum oven (200 mmHg, 40°C) for 3 h. Afterward, the SPR chip was immersed in ethanol/water (4 : 1, v/v) solution containing 3.0 *M* allyl mercaptan for 12 h. Then, it was rinsed with ethanol and dried with N_2 under vacuum (200 mmHg, 40°C).

To attach the CAP imprinted nanoparticles onto the allyl mercaptan modified SPR chip, an aliquot (5 μL) of nanoparticle dispersion (4.2%, v/v) was dropped on the gold surface of the SPR sensor. Then, the SPR chip was dried in oven at 37°C for 6 h meanwhile UV-radiation (365 nm, 100 W) was applied (Supporting Information Figure SI-1). Finally, the CAP imprinted SPR nanosensor was washed several times with ethyl alcohol, ethyl alcohol : water mixture (75 : 25; 50 : 50; 25 : 75, v:v) and finally deionized water and then dried with N_2 under vacuum (200 mmHg, 40°C).

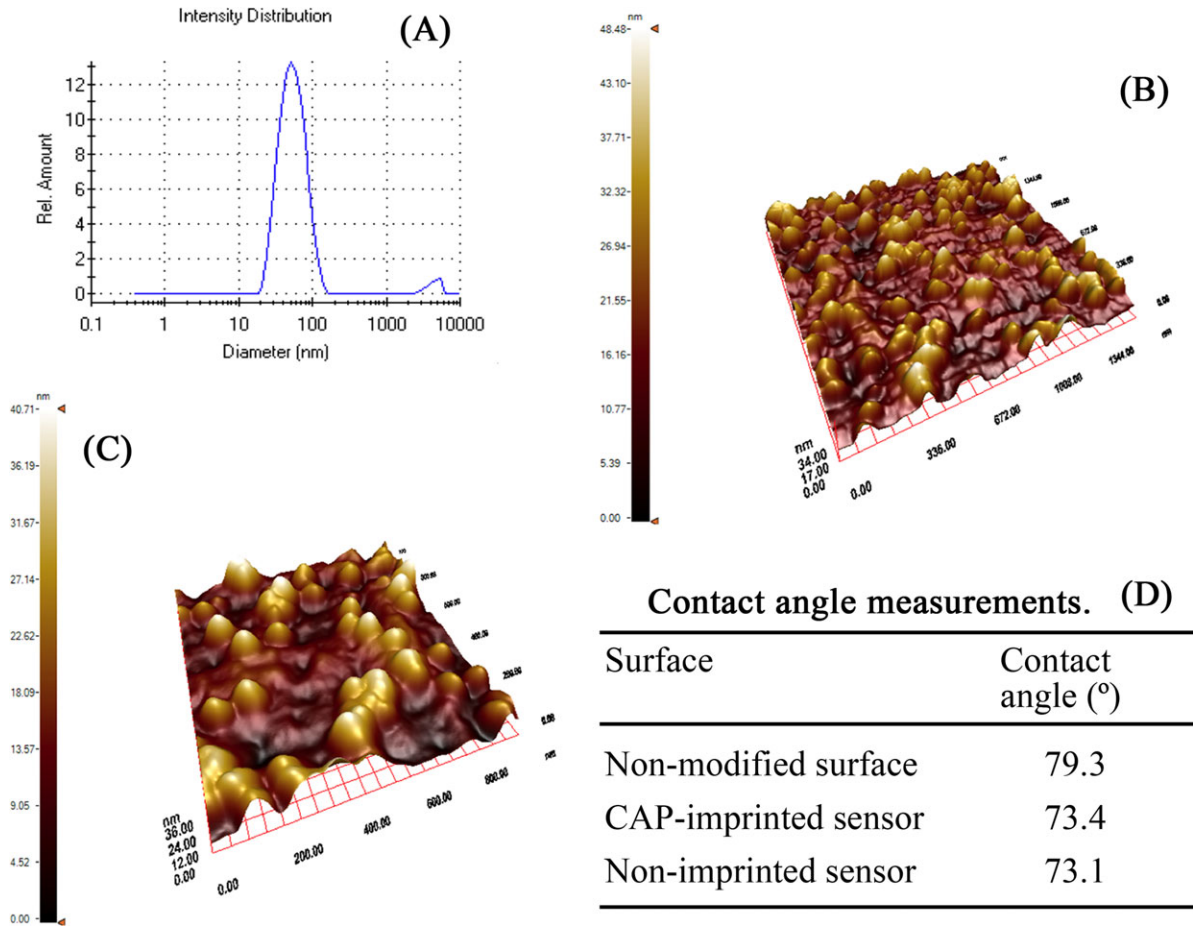

Contact angle measurements. (D)

Surface	Contact angle (°)
Non-modified surface	79.3
CAP-imprinted sensor	73.4
Non-imprinted sensor	73.1

Figure 1. Characterization of CAP imprinted nanosensor. (A) Zeta-size results of CAP imprinted nanoparticles; (B) AFM image of CAP imprinted SPR nanosensor; (C) AFM image of NIP SPR nanosensor; (D) contact angle measurements of the SPR nanosensor. [Color figure can be viewed in the online issue, which is available at wileyonlinelibrary.com.]

Template Removal from SPR Nanosensor

To remove template molecule, ultra pure water was used as desorption agent. The first removal step was carried out via batch experimental setup. The CAP imprinted SPR nanosensor was immersed into desorption solution (ethyl acetate, 20 mL) and shaked in a bath (200 rpm) at room temperature for 2 h. After CAP removal, the nanosensor was dried in oven and kept dust-free environment until use.

Surface Characterization of CAP Imprinted SPR Nanosensor

Atomic force microscopy (AFM) equipment (Nanomagnetics Instruments, Oxford, UK) was used for surface characterization of the SPR nanosensor. AFM yields the images in high resolution (up to 4096 × 4096 pixels) because of free cantilever interferometer. The CAP imprinted SPR nanosensor was attached on a sample holder by using double-side carbon strip. Observation was carried out under ambient condition. Applied experimental parameters were oscillation frequency (341.30 Hz), vibration amplitude (1 V_{RMS}), and free vibration amplitude (2 V_{RMS}). Samples were scanned with 2 μm/s scanning rate and 256 × 256 pixels resolution to obtain a view of 2 μm × 2 μm area.

Contact angle of the SPR nanosensor was determined with KRUSS DSA100 (Hamburg, Germany) instrument. Contact angle of the chip surface was measured with sessile drop method by dripping of water. Ten separate photos were taken from the different parts of chip surface; later, contact angle values were measured for each drop. Measured contact angle values were obtained as the left contact angle, the angles from the left contact point of the droplet with solid and right contact angle, from the right contact point of the droplet with solid. In addition, average contact angle values were obtained and reported as the average of two values.

Kinetic Studies with SPR Nanosensor

After preparation of the CAP imprinted SPR nanosensor, kinetic studies were performed for real-time detection of CAP from aqueous solution with a SPR system (GenOptics, Orsay, France). Gold-coated (thickness 50 nm) SPR chips (25 mm × 12.5 mm) were also supplied from GenOptics. The CAP imprinted SPR nanosensor was washed with deionized water (50 mL, 2.0 mL/min flow rate) and equilibration buffer (pH 7.2, phosphate buffer, 50 mL, 2.0 mL/min flow rate). Then, the CAP solutions in concentration range of 0.155–6.192 n*M* were applied to the SPR system (10 mL and 2.0 mL/min flow rate). The changes in resonance frequency were monitored real time and reached to platue at about 10 min. After that, desorption was done by applying 10 mL of ultra pure water at the flow rate of 1.0 mL/min. After the end of desorption step, CAP imprinted SPR nanosensor was washed with deionized water and equilibration buffer. Adsorption–

desorption–cleaning steps were repeated for each CAP sample, meanwhile, SPR1001 software obtained from producer was used to analyze the kinetic data. Honey samples from local markets were used in spiking studies. CAP extraction from honey samples carried out according to related literature[35] could be summarized as: 5.0 ± 0.02 g of honey was mixed with 10 mL extraction buffer and then, 12 mL of ethyl acetate was added. After mixing 30 min on a rolling mixer, centrifugation at 2150 × *g* for 10 min was performed. Then, 8 mL of the organic layer was transferred to a test tube and evaporated until drying under nitrogen atmosphere on a sample concentrator at 70°C. The residue was reconstituted in 10 mL of phosphate buffer (pH 7.2) and ethanol in ratio of 9/1 (v/v). Honey samples were spiked with CAP (25–200 μL, 0.1 *M*) for validation purposes. The specificity of the CAP imprinted SPR nanosensor was tested using the NIP SPR nanosensor via using TAP and FLP as competitors.

RESULTS AND DISCUSSIONS

Preparation and Characterization of CAP Imprinted Nanoparticles

Two-phase miniemulsion polymerization method was used to prepare the CAP imprinted PEDMAH nanoparticles. Characterization of the nanoparticles was performed by zeta-sizer measurement. According to results of zeta-sizer measurements, average particle size of CAP imprinted nanoparticles was estimated as 52 nm with polydispersity index around 0.205 [Figure 1(A)].

After attachment of the nanoparticles onto the SPR chip surface, SPR nanosensors were characterized by AFM. 3D AFM images of the CAP imprinted and the NIP nanosensors were presented in Figure 1(B,C). Surface deepness of bare sensor surface was 7.37 nm. After attachment of nanoparticles onto the sensor surface, surface deepness of the CAP imprinted nanosensor increased to 48.48 nm and that of the NIP nanosensor increased to 40.71 nm. These results showed that surface roughness increased and attachment of nanoparticles onto the SPR chip surface was successfully achieved. As regards to 3D AFM images, it is understood that homogenous and monolayer attachment of nanoparticles was accomplished. Contact angles of SPR chips were presented in Figure 1(D). As seen in the figure, contact angle of both MIP and NIP nanosensors decreased from 79.3° to 73.4° and 73.1°, respectively. In our study, the decrease in contact angles indicated the increase in surface hydrophilicity of the prepared nanosensors, which enhanced the wettability of sensor surface and plasmon formation.

Kinetic Studies with SPR Nanosensor

Compared to conventional bulk imprinting process, imprinted nanoparticles have some remarkable advantages. First, imprinted molecular cavities in nanoparticles can be obtained as more homogeneously distributed than obtained in bulk-imprinted particles.[36] Second, imprinted molecular cavities can be obtained at the surface or near inside of the nanoparticles so that the template molecules can be removed easily.[32] Therefore, rapid and homogenous adsorption dynamics can be achieved meanwhile higher adsorption capacities and rates can be obtained by increasing the number of accessible cavities.[34,37] In our study, the CAP imprinted nanosensor was used for real-time detection of CAP from aqueous solutions in the concentration range of 0.155–6.192 n*M*. Real-time change in SPR nanosensor response with respect to time was given in Figure 2(A). As seen in figure, Δ*R* values increased with increasing concentration of CAP solutions as expected. All steps were almost completed in 42 min. At the beginning, response of SPR nanosensor increased and then reached the plateau value around 3.0 n*M* because of saturation of accessible imprinted nanocavities.

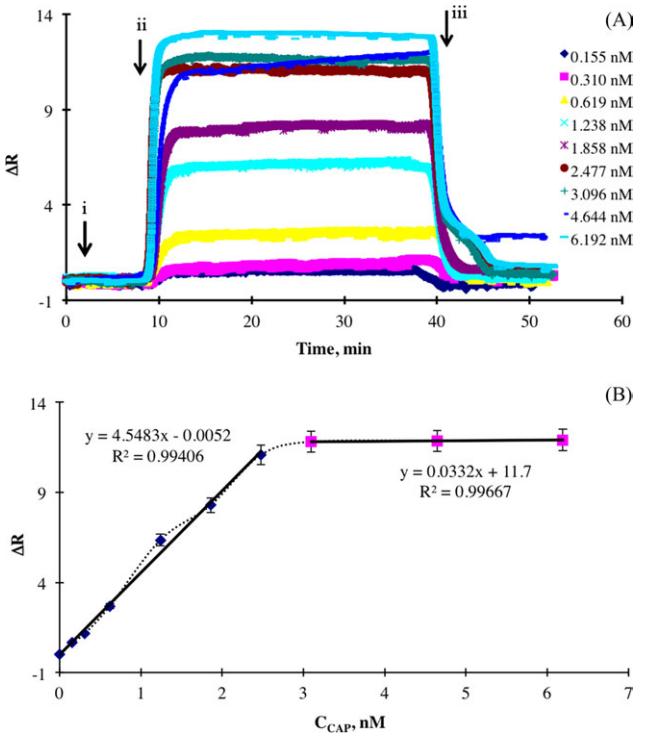

Figure 2. Real-time CAP detection with CAP imprinted SPR nanosensor. (A) The sensorgrams of interaction between different concentrations of CAP and imprinted SPR nanosensors, Δ*R* vs. time; (B) concentration vs. nanosensor response. [Color figure can be viewed in the online issue, which is available at wileyonlinelibrary.com.]

Relationship between concentration of CAP and Δ*R* was given in Figure 2(B). According to Figure 2(B), the SPR nanosensor response reached maximum value at 3.096 n*M* concentration of CAP. The CAP imprinted SPR nanosensor has two different linear regions between 0–2.477 n*M* and 3.096–6.192 n*M* concentrations with R^2 values of 0.99406 and 0.99667, respectively. These results showed that CAP molecules bound to the CAP imprinted SPR nanosensor through two different orientations with high affinity.[36]

Equilibrium Isotherm Models Application for Data Analysis

To describe the detection system and to analyze the interaction kinetics between the CAP imprinted SPR nanosensor and the analyte molecules, five models including association kinetic analysis and Scatchard, Langmuir, Freundlich, and Langmuir-Freundlich models were applied to biosensing data.

$$\text{Scatchard}\quad \Delta R_{ex}/C = K_A(\Delta R_{max} - \Delta R_{eq}) \tag{1}$$

$$\text{Langmuir}\quad \Delta R = \{\Delta R_{max} C/K_D + C\} \tag{2}$$

$$\text{Freundlich}\quad \Delta R = \Delta R_{max} C^{1/n} \tag{3}$$

$$\text{Langmuir} - \text{Freundlich}\quad \Delta R = \{\Delta R_{max} C^{1/n}/K_D + C^{1/n}\} \tag{4}$$

Table I. Kinetic and Isotherm Parameters

Association kinetic analysis		Equilibrium analysis (Scatchard)	
k_a (nM/min)	1.0328	ΔR_{max}	12.01
k_d (1/min)	0.2951	K_A (nM)	18.1
K_A (nM)	3.50	K_D (1/nM)	0.055
K_D (1/nM)	0.286	R^2	0.9395
R^2	0.9593		

Langmuir		Freundlich		Langmuir-Freundlich	
ΔR_{max}	83.33	ΔR_{max}	3.87	ΔR_{max}	24.57
K_A (nM)	0.051	$1/n$	0.8594	$1/n$	0.8594
K_D (1/nM)	19.69	R^2	0.9442	K_D (1/nM)	7.656
R^2	0.9941			K_A (nM)	0.131
				R^2	0.9925

where $d\Delta R/dt$ is the rate of change of the SPR response, ΔR and ΔR_{max} are experimental and theoretical maximum sensor responses measured while binding of analyte molecule (reflectivity%/s), C is the injected concentration (nM), k_a is the association rate constant (1/nM s), k_d is the dissociation rate constant (1/s), $1/n$ is Freundlich heterogeneity index. Binding constant, that is, association constant K_A, may be calculated as $K_A = k_a/k_d$ (1/nM) and dissociation constant, K_D (nM), is equal to $1/K_A$.

The adsorption models were used to determine surface homogeneity of the imprinted materials. Langmuir model bases on the assumptions of homogeneous distribution of interaction points with equal energy and no lateral interactions. Freundlich model is well fitted to heterogeneous surfaces. Mixed model, Langmuir-Freundlich can be applied to a system not completely fitted to both systems, provides heterogeneity information adsorption behavior over wide concentration regions. Scatchard, Langmuir, Freundlich, and Langmuir–Freundlich models were applied to experimental data. The calculated parameters for all applied models are given in Table I. R^2 values obtained from Langmuir and Langmuir-Freundlich models were higher than those of R^2 values obtained from Scatchard and Freundlich. However, the highest R^2 value (0.9941) was found for Langmuir model. This means that Langmuir equation is the best-fitted model to explain the interaction between the SPR nanosensor and the CAP molecules. In other words, binding of the CAP molecules onto the SPR nanosensor was monolayer although Scatchard curve showed some surface heterogeneity. Their surface heterogeneity can be occurred because of accessibility problem of imprinted nanocavities due to attachment on the SPR nanosensor surface. But, these nanocavities still show high

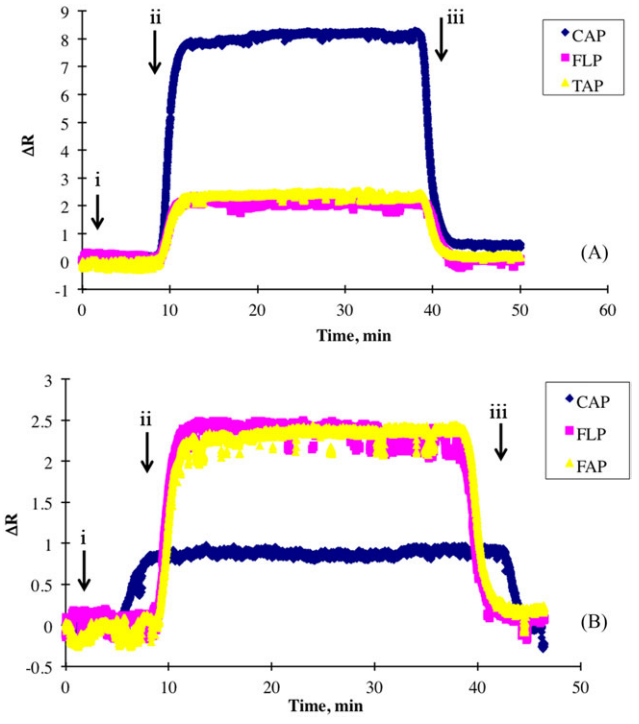

Figure 3. The selectivity of CAP imprinted nanosensor. Competition of CAP with FLP and TAP molecules. (A) CAP imprinted; (B) NIP SPR nanosensor. (i) Equilibration with phosphate buffer (pH 7.2); (ii) injection of antibiotic molecules (concentration for each 1.858 nM); (iii) desorption with ultra pure water. [Color figure can be viewed in the online issue, which is available at wileyonlinelibrary.com.]

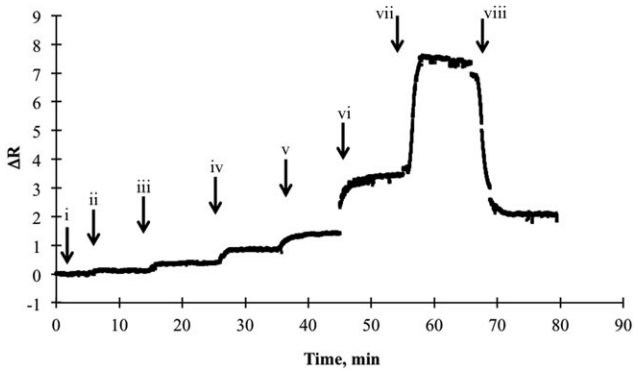

Figure 4. Real-time CAP detection from honey sample. (i) Equilibration with phosphate buffer (pH 7.2); (ii) injection of honey extract; (iii) injection of honey extract spiked with CAP (25 μL, 0.1 M); (iv) injection of honey extract spiked with CAP (50 μL, 0.1 M); (v) injection of honey extract spiked with CAP (75 μL, 0.1 M); (vi) injection of honey extract spiked with CAP (100 μL, 0.1 M); (vii) injection of honey extract spiked with CAP (200 μL, 0.1 M); (viii) desorption with ultra pure water.

affinity to CAP molecules. Detection limit, defined as the concentration of analyte giving reflectivity shift equivalent to three standard deviations of the blank, was determined as 40 ng/kg honey.

Specificity and Selectivity of CAP Imprinted SPR Nanosensor

Selectivity studies of the CAP imprinted SPR nanosensor were performed with structurally similar compounds TAP and FLP. For testing of selectivity of SPR nanosensor, the solutions containing 1.858 n*M* of CAP, TAP, and FLP were passed through the surface of the CAP imprinted and the NIP nanosensors. The responses of MIP nanosensor in solutions of 1.858 n*M* CAP, TAP, and FLP were given in Figure 3(A). As seen in the figure, the nanosensor response of CAP was notably higher than that of TAP and FLP. TAP and FLP showed low and nonspecific responses. These responses were possibly resulted from structural and physico-chemical similarities of TAP and FLP to CAP molecules. The responses of CAP imprinted nanosensor to CAP, TAP, and FLP were 8.2837, 2.3385, and 2.5386, respectively. The selectivity ratios calculated by dividing SPR response to those of competitor molecules TAP and FLP were 3.54 and 3.26, respectively. These data showed that adsorption of CAP molecules to the nanoparticles is much more than those of competitive agents. To confirm both selectivity and specificity of the CAP imprinted SPR nanosensor, the NIP nanosensor was also prepared and used for real-time TAP and FLP detection studies [Figure 3(B)]. The responses of the NIP nanosensor to CAP, TAP, and FLP molecules were 0.9807, 2.447, and 2.494, respectively. The selectivity ratios for TAP and FLP were 0.40 and 0.39, respectively. Relative selectivity coefficient for TAP was 8.86 and for FLP was 8.36. These values mean that the CAP imprinted nanoparticles recognize CAP molecules 8.86 times more than do TAP molecules and 8.36 times more than do FLP molecules. It could be concluded that the CAP imprinted SPR nanosensor specifically detects CAP molecule. The CAP imprinted SPR nanosensor was also used to detect CAP in honey samples. For this purpose, the honey samples, unspiked and spiked with CAP solution (25–200 μL, 0.1 *M*) were interacted with the CAP imprinted SPR nanosensor (Figure 4). As seen in the figure, the CAP imprinted SPR nanosensor showed quick response whenever spiked honey sample reached sensor surface whereas there was no significant response for unspiked honey sample. Here, it should specially be mentioned that the response of the sensor is reproducible and increased with increasing CAP amount spiked into honey sample. As a result, the CAP imprinted SPR nanosensor is potential candidate for real-time CAP determination in honey sample.

CONCLUSIONS

We developed a SPR nanosensor for real-time detection of CAP by using molecular imprinting technique. The CAP imprinted nanoparticles were prepared in the presence of MAH and EDMA by miniemulsion polymerization. To check over, the NIP nanoparticles were also prepared without CAP. The CAP imprinted nanoparticles were characterized by zeta-sizer and average particle size of the imprinted nanoparticles was determined as 52 nm. Then, the PEDMAH nanoparticles were attached onto the surface of gold SPR chip. AFM and contact angle measurements were performed for the surface characterization. The results indicated that homogenous and monolayer attachment of nanoparticles was accomplished. According to the kinetic studies and adsorption isotherms, Langmuir model was found the most appropriate adsorption model for this system. The detection limit was found as 40 ng/kg honey sample. FLP and TAP were chosen as competitors to determine selectivity of nanoparticles. The imprinted nanoparticles selectively recognized the CAP molecules 8.86 times more than TAP and 8.36 times more than FLP. The CAP imprinted SPR nanosensor shows reproducible results for honey samples spiked with CAP, and the SPR nanosensor response increased with increasing CAP amount spiked. It can be concluded that the CAP imprinted SPR nanosensor has a potential use for food safety purposes.

ACKNOWLEDGEMENT

This study was financially supported by Karadeniz Technical University with a project number of 2008.101.002.2.

REFERENCES

1. U.S. Department of Health and Human Services. Report on Carcinogens, 11th ed.; U.S. Department of Health and Human Services: Washington, DC, **2011**, p 92.
2. Dawson, S.; Elliot, J.; Taylor, M. A., In The Veterinary Formulary; Bishop, Y., Ed.; The University Press, The British Veterinary Association: Cambridge, UK, **2005**, p 139.
3. Fodey, T.; Murilla, G.; Cannavan, A.; Elliott, C. *Anal. Chim. Acta* **2007**, *592*, 51.
4. European Commission. *Official J. Eur. Commun.* **1990**, *L224*, 1.
5. European Commission. *Official J. Eur. Commun.* **1994**, *L156*, 6.
6. Fedorova, M. D.; Andreeva, I. P.; Vilegzhanina, E. S.; Komarov, A. A.; Rubtsova, Y. M.; Samsonova, J. V.; Egorov, A. M. *Appl. Biochem. Microbiol.* **2010**, *46*, 795.
7. Hanekamp, J. C.; Frapporti, G.; Olieman, K. *Environ. Liability* **2003**, *6*, 209.
8. European Commission. *Official J. Eur. Commun.* **2003**, *L71*, 17.
9. Tajik, H.; Malekinejad, H.; Razavi-Rouhani, S. M.; Pajouhi, M. R.; Mahmoudi, R.; Haghnazari, A. *Food Chem. Toxicol.* **2010**, *48*, 2464.
10. Berendsen, B. J. A.; Zuidema, T.; de Jong, J.; Stolker, L. A. M.; Nielen, M. W. F. *Anal. Chim. Acta* **2011**, *700*, 78.
11. Sai, N.; Chen, Y.; Liu, N.; Yu, G.; Su, P.; Feng, Y.; Zhou, Z.; Liu, X.; Zhou, H.; Gao, Z.; Ning, B. A. *Talanta* **2010**, *82*, 1113.
12. Shakila, R. J.; Saravanakumar, R.; Vyla, S. A. P.; Jeyasekaran, G. *Innov. Food Sci. Emerg. Technol.* **2007**, *8*, 515.
13. Jin, W.; Ye, X.; Yu, D.; Dong, Q. *J. Chromatogr. B* **2000**, *741*, 155.
14. Thongchai, W.; Liawruangath, B.; Liawruangrath, S.; Greenway, G. M. *Talanta* **2010**, *82*, 560.
15. Zhang, N.; Xiao, F.; Bai, J.; Lai, Y.; Hou, J.; Xian, Y.; Jin, L. *Talanta* **2011**, *87*, 100.

16. Zhang, S.; Zhou, J.; Shen, J.; Ding, S.; Li, J. *J. AOAC Int.* **2006**, *89*, 369.
17. Petz, M. *Monatshefte für Chemie/Chem. Month.* **2009**, *140*, 953.
18. Uzun, L.; Say, R.; Unal, S.; Denizli, A. *Biosens. Bioelectron.* **2009**, *24*, 2878.
19. Diltemiz, S. E.; Denizli, A.; Ersöz, A.; Say, R. *Sens. Actuat. B* **2008**, *133*, 484.
20. Chen, H.; Cheng, H.; Lee, J.; Kim, J. H.; Hyun, M. H.; Koh, K. *Talanta* **2008**, *76*, 49.
21. Hu, C.; Gan, N.; Chen, Y.; Bi, L.; Zhang, X.; Song, L. *Talanta* **2009**, *80*, 407.
22. Baumgarten, S.; Robelek, R. *Sens. Actuat. B* **2011**, *156*, 798.
23. Homola, J. *Chem. Rev.* **2008**, *108*, 462.
24. Whitcombe, M. J.; Chianella, I.; Larcombe, L.; Piletsky, S. A.; Noble, J.; Porter, R.; Horgan, A. *Chem. Soc. Rev.* **2011**, *40*, 1547.
25. Homola, J.; Yee, S. S.; Myszka, D. In Optical Biosensors: Present and Future; Ligler, F. S.; Taitt, C. R., Eds.; Elsevier B.V.: Amsterdam, NL, **2002**, p 207.
26. Uzun, L.; Say, R.; Unal, S.; Denizli, A. *J. Chromatogr. B* **2009**, *877*, 181.
27. Erturk, G.; Uzun, L.; Tumer, M. A.; Say, R.; Denizli, A. *Biosens. Bioelectron.* **2011**, *28*, 97.
28. Weia, C.; Zhoub, H.; Zhou, J. *Talanta* **2011**, *83*, 1422.
29. Chen, L.; Xu, S.; Li, J. *Chem. Soc. Rev.* **2011**, *40*, 2922.
30. Bereli, N.; Andac, M.; Baydemir, G.; Say, R.; Galaev, I. Y.; Denizli, A. *J. Chromatogr. A.* **2008**, *1190*, 18.
31. Tamahkar, E.; Bereli, N.; Say, R.; Denizli, A. *J. Sep. Sci.* **2011**, *34*, 3433.
32. Asliyuce, S.; Uzun, L.; Rad, A. Y.; Unal, S.; Say, R.; Denizli, A. *J. Chromatogr. B* **2012**, *889–890*, 95.
33. Poma, A.; Turner, A. P. F.; Piletsky, S. A. *Trend Biotechnol.* **2010**, *28*, 629.
34. Sener, G.; Ozgur, E.; Yilmaz, E.; Uzun, L., Say, R.; Denizli, A. *Biosens. Bioelectron.* **2010**, *26*, 815.
35. Ferguson, J.; Baxter, A.; Young, P.; Kennedy, G.; Elliott, C.; Weigel, S.; Gatermann, R.; Ashwin, H.; Stead, S.; Sharman, M. *Anal. Chim. Acta* **2005**, *529*, 109.
36. Sener, G.; Uzun, L.; Say, R.; Denizli, A. *Sens. Actuat. B* **2011**, *160*, 791.
37. Bossi, A.; Bonini, F.; Turner, A. P. F. and Piletsky, S. A. *Biosens. Bioelectron.* **2007**, *22*, 1131.